

Adaptation and Performance of the Cartesian Coordinates Fast Multipole Method for Nanomagnetic Simulations

Wen Zhang, Stephan Haas

*Department of Physics and Astronomy, University of Southern California
Los Angeles, CA 90089, USA*

Abstract

An implementation of the fast multiple method (FMM) is performed for magnetic systems with long-ranged dipolar interactions. Expansion in spherical harmonics of the original FMM is replaced by expansion of polynomials in Cartesian coordinates, which is considerably simpler. Under open boundary conditions, an expression for multipole moments of point dipoles in a cell is derived. These make the program appropriate for nanomagnetic simulations, including magnetic nanoparticles and ferrofluids. The performance is optimized in terms of cell size and parameter set (expansion order and opening angle) and the trade off between computing time and accuracy is quantitatively studied. A rule of thumb is proposed to decide the appropriate average number of dipoles in the smallest cells, and an optimal choice of parameter set is suggested. Finally, the superiority of Cartesian coordinate FMM is demonstrated by comparison to spherical harmonics FMM and FFT.

Key words: FMM, cartesian, magnet

PACS: 02.70.-c, 75.75.+a

1. Introduction

Magnetic nanoparticles and fluids have attracted intensive investigation during the last two decades [1, 2, 3, 4, 5]. Micromagnetic simulation is a powerful tool to study such systems, where the main challenge is the dipolar

Email address: zhangwen@usc.edu (Wen Zhang)

interaction between magnetic moments, which can be dealt with either discretely or in the continuum limit. Since the interaction is long ranged, the complexity of a brute-force calculation will be $\mathcal{O}(N^2)$. One popular method to improve this performance is by Fast Fourier Transform (FFT), which reduces the complexity to $\mathcal{O}(N * \log(N))$. However, FFT suffers from the fact that it requires a regular lattice arrangement of dipoles, and a large number of padding areas have to be added when dealing with exotic geometries and open boundary conditions. Thus, the alternative, fast multipole method (FMM) has attracted increasingly more attention in the past several years [6, 7, 8, 9].

The FMM was first introduced by L. Greengard *et al* [10, 11], and has been used ever since to speed up large scale simulations involving long ranged interactions. It has the charming advantage of $\mathcal{O}(N)$ complexity. Furthermore, there is no constraint on the distribution of particles and the boundaries of the system. Hence it is extremely useful for magnetic fluid systems and nanomagnets with exotic geometries. Last but not least, it is a scalable algorithm, i.e. it can be efficiently implemented in parallel [12]. With so many advantages though, the adoption of FMM in magnetic system is not widely applied, probably due to two reasons. One concern is that since there is a huge overhead to achieve $\mathcal{O}(N)$ complexity, the FMM becomes faster only for very large N . Actually this is true only when one considers a very high order expansion (say 10). In the context of micromagnetics, we will show that an expansion to the order of no more than 6 will be satisfying, and with some optimization procedure FMM will be superior even in a system of 10^3 dipoles. The other reason is that the standard implementation of the FMM algorithm is based on the well-known spherical harmonics expansion [13] of $1/r$. For dipolar interaction which decays as $1/r^2$, however, it is not straightforward to apply. Further, the additional complexity of calculating spherical harmonics acts as another barrier. To overcome these shortcomings, expansions in Cartesian coordinate were proposed [14, 15], but they were not applied successfully until recently [8]. Following these studies, here we present a very simple but useful formula (Eq. 3) to calculate the multipole moments in dipolar systems.

In Section II and III, a brief description of the FMM algorithm and all the necessary equations is presented. In Section IV, performance issues will be discussed in detail. The number of dipoles contained in the smallest cell will be shown to be crucial in terms of performance and a rule of thumb on choosing the right number will be given (Eq. 17). Then, the optimal choice

of expansion order and opening angle to achieve certain error bounds will be discussed, followed by quantitative study of the trade off between computing time and accuracy. Finally, we compare the Cartesian coordinates FMM with spherical harmonics FMM and FFT.

2. Algorithm

The crucial ideas of the FMM are: (i) chunk source points together into large cells whose field in remote cells is computed by a multipole expansion of the source points; (ii) use a single Taylor expansion to express the smooth field in a given cell contributed by the multiple expansions of all remote cells. As the details of the algorithm are discussed in previous literature [10, 7], here we will only briefly describe them, stressing those aspects which are special to our implementation. Instead of the regular geometric hierarchical traversals of the system, we follow a simple alternative way[7] by using recursive functions. This method simplifies the program significantly and is especially elegant for system with exotic geometries, since one only needs to recursively divide the system into halves.

After setting up all the cells, the entire program mainly consists of three recursive functions traversing the entire system trice. Pseudocodes are provided in the Appendix.

1. Downward Pass: construct “partners” list (similar to the interaction list in the original FMM [10]). For each cell, the partners list contain those cells which are near to its parent but far to itself. Instead of the original geometric rules (near cell pairs are those cells touching each other), near cell pairs refer to those with opening angle α larger than certain value α_m ($\alpha_m < 1$). The opening angle is defined as $2r/d$ ($\alpha_m \equiv 2r/d$), where r is the “radius” of two cells and d is the distance between their centers. Note that “radius” denotes the maximum distance between a corner of one cell and its center. With these definitions, it is easy to construct the partners lists. First, set the partners list of each cell to be empty. Then, for each cell except those cells without children (leaf cells), start from its partners list generated by its parent (for the root cell, this list is empty) and perform the following procedure: (i) add the children of all its near cells it to the partners list of each of its children, and delete these cells from its own partners list; (ii) add one of its children to the other child’s partners list (do it for both children); (iii) call its children to perform these tasks. In this way, we start from the root cell and recursively traverse its children until reaching leaf

cells. For each leaf cell, add to another list called “nearPartners” those cells in the partners list which are near to it and delete them from its partners list. Finally put itself in its nearPartners list.

2. Upward Pass: construct the multipole moments for each cell. Start from the leaf cells and explicitly calculate their multipole moments according to Eq. 3 below. Then upward traverse all the other cells in binary tree hierarchy whose multipole moments are obtained by shifting the origin of its children’s multipole moments (see Eq. 7). This process can be easily realized by a recursive function.

3. Downward Pass: construct the Taylor expansion of the smooth field in each cell. Start from the root cell and down traverse all the other cells in the binary tree hierarchy. For each cell, inherit the Taylor expansion coefficients of the smooth field from its parents according to Eq. 10 and then add to it the contribution from the cells in the partners list according to Eq. 11.

After these three steps, the only contributions to the magnetostatic field that are not counted come from dipole pairs among the leaf cells which are near to each other or within the same cell. So for each field point in the leaf cell, calculate explicitly Eq. 16, which sum over all the dipoles in those cells in the nearPartners list except the very dipole located at the field point.

In the majority of implementations of the FMM, the potential is expanded in terms of spherical harmonics, which complicates the code and requires long computing time. Previous attempts were made to expand in Cartesian coordinates [14, 15, 7]. Initially, the expansion coefficients were calculated either by hand or in a computationally inefficient way, but they can in fact be obtained very fast nowadays[7] using Eqs. 12 and 13. The disadvantage of Cartesian expansion is that the number of terms below each order is larger than that with spherical harmonics, but this inefficiency is less than a factor of two up to order 8. We will show later that in most cases in the micromagnetic simulation, an order of no more than 6 is sufficient.

3. Formalism

In this section, we provide all the necessary formulae to implement the above algorithm for nanomagnetic simulation, following Ref. [7]. To simplify the formalism, the following shorthand notations are defined:

$$\begin{aligned} \mathbf{n} &\equiv (n_x, n_y, n_z) \\ n &\equiv n_x + n_y + n_z \end{aligned}$$

$$\begin{aligned}\mathbf{r}^{\mathbf{n}} &\equiv x^{n_x} y^{n_y} z^{n_z} \\ \mathbf{n}! &\equiv n_x! n_y! n_z!\end{aligned}\tag{1}$$

Define the multipole moments of a given charge distribution q_i :

$$Q_{\mathbf{n}} = \frac{1}{\mathbf{n}!} \sum_i q_i \mathbf{r}_i^{\mathbf{n}}.\tag{2}$$

The evaluation of $Q_{\mathbf{n}}$ is straightforward for monopoles. For dipoles, however, this is not the case. One way to proceed is divide the system always into cells which contain only one dipole at the center, based on the fact that only $Q_{(1,0,0)}$, $Q_{(0,1,0)}$ and $Q_{(0,0,1)}$ survive for a single dipole \vec{m} located at the origin, and they equal m_x , m_y and m_z respectively. Nevertheless, this method is not convenient and even inapplicable for certain systems like ferrofluids. Moreover, having multiple dipoles in each leaf cell has performance advantages. This issue will be discussed in detail in Sec IV. Thus it is important to have an easy formula to calculate multipole moments for dipolar system. Previous studies have shown complicated formulas for spherical harmonics expansion [9]. For the multipole moments in Cartesian coordinate, it becomes much simpler, i.e.

$$Q_{\mathbf{n}} = \frac{1}{\mathbf{n}!} \sum_i \vec{m}_i \cdot \nabla \mathbf{r}_i^{\mathbf{n}}.\tag{3}$$

In order to derive this formula, we follow the standard procedure to treat a dipole $\vec{m}(\vec{r})$ as a limit of two point monopoles $\pm q$ located at $\vec{r} \pm \vec{d}$ when $d \rightarrow 0$, keeping $\vec{m} = 2q\vec{d}$. After Taylor expansion, Eq. 3 appears.

If $1/|\vec{r} - \vec{r}_i|$ is expanded in Taylor series at r_i , the potential $V(\vec{r}) = \sum_i q_i/|\vec{r} - \vec{r}_i|$ can be expressed in a compact form in terms of the multipole moments,

$$\frac{1}{|\vec{r} - \vec{r}_i|} = \sum_{\mathbf{n}} \frac{1}{\mathbf{n}!} D_{\mathbf{n}}(\vec{r}) \mathbf{r}^{\mathbf{n}},\tag{4}$$

$$D_{\mathbf{n}}(\vec{r}) \equiv \frac{\partial^{\mathbf{n}}}{\partial (-\mathbf{r})^{\mathbf{n}}} \left(\frac{1}{|\vec{r}|} \right),\tag{5}$$

$$V(\vec{r}) = \sum_{\mathbf{n}} D_{\mathbf{n}}(\vec{r}) Q_{\mathbf{n}}.\tag{6}$$

In the upward pass (step 2), one needs to shift the origin of the multipole moments. The moments $Q_{\mathbf{n}}$ about the origin O are related to $Q'_{\mathbf{n}}$ about position \vec{c} (with respect to O) by

$$Q_{\mathbf{n}} = \sum_{\mathbf{p}} \frac{\mathbf{c}^{\mathbf{p}}}{\mathbf{p}!} Q'_{\mathbf{n}-\mathbf{p}}. \quad (7)$$

The Taylor expansion of an arbitrary potential function $V(\vec{r})$ is:

$$V(\vec{r}) = \sum_{\mathbf{n}} \frac{1}{\mathbf{n}!} V_{\mathbf{n}} \mathbf{r}^{\mathbf{n}}, \quad (8)$$

$$V_{\mathbf{n}} \equiv \frac{\partial^{\mathbf{n}}}{\partial \mathbf{r}^{\mathbf{n}}} V(\vec{r})|_{\vec{r}=0}. \quad (9)$$

In the second downward pass (step 3), one needs to shift the origin of the $V_{\mathbf{n}}$ when a child inherits $V_{\mathbf{n}}$ from its parent. The child's $V'_{\mathbf{n}}$ about position \vec{c} (with respect to its parent's origin O) is related to its parent's $V_{\mathbf{n}}$ by

$$V'_{\mathbf{n}} = \sum_{\mathbf{p}} \frac{\mathbf{c}^{\mathbf{p}}}{\mathbf{p}!} V_{\mathbf{n}+\mathbf{p}} \quad (10)$$

Besides, one also needs to calculate the Taylor expansion coefficient in a given cell from its partner's multipole moments. This is achieved by

$$V_{\mathbf{n}} = (-1)^n \sum_{\mathbf{p}} D_{\mathbf{n}+\mathbf{p}}(\vec{c}) Q_{\mathbf{p}}, \quad (11)$$

where \vec{c} is the position vector of the center of this cell with respect to the center of its partner whose multipole expansion is $Q_{\mathbf{p}}$. It can be shown [7] that $D_{\mathbf{n}}(\vec{r})$ has the form:

$$D_{\mathbf{n}}(\vec{r}) = \frac{1}{r^{2n+1}} \sum_{\mathbf{p}(p=n)} F_{\mathbf{n}}(\mathbf{p}) \mathbf{r}^{\mathbf{p}} \quad (12)$$

Thus the problem of calculating $D_{\mathbf{n}}$ breaks down to creating the table $F_{\mathbf{n}}(\mathbf{p})$. Note that by definition of $D_{\mathbf{n}}$, we have: can be calculated by $D_{\mathbf{n}}$.

$$D_{\mathbf{n}+\hat{\mathbf{x}}}(\vec{r}) = -\frac{\partial}{\partial x} D_{\mathbf{n}}$$

$$\begin{aligned}
&= \frac{1}{r^{2n+3}} \sum_{\mathbf{p}} F_{\mathbf{n}}(\mathbf{p}) (-p_x \mathbf{r}^{\mathbf{p}-\hat{\mathbf{x}}+2\hat{\mathbf{y}}} \\
&\quad - p_x \mathbf{r}^{\mathbf{p}-\hat{\mathbf{x}}+2\hat{\mathbf{z}}} + (2n+1-p_x) \mathbf{r}^{\mathbf{p}+\hat{\mathbf{x}}})
\end{aligned} \tag{13}$$

where $\hat{x} = (1, 0, 0)$. Meanwhile according to Eq. 12,

$$D_{\mathbf{n}+\hat{\mathbf{x}}}(\vec{r}) = \frac{1}{r^{2n+3}} \sum_{\mathbf{p}'(p'=n+\hat{x})} F_{\mathbf{n}+\hat{\mathbf{x}}}(\mathbf{p}') \mathbf{r}^{\mathbf{p}'} \tag{14}$$

Similarly one can obtain the such formulas for $D_{\mathbf{n}+\hat{\mathbf{y}}}$ and $D_{\mathbf{n}+\hat{\mathbf{z}}}$ (a permutation through x, y, z in above equations). Therefore each \mathbf{n} , $F_{\mathbf{n}}(\mathbf{p})$ can clearly be built from $F_{\mathbf{n}-\hat{\nu}}(\mathbf{p})$ recursively starting from $F_{(0,0,0)}((0,0,0)) = 1$, where ν is chosen among x, y, z such that $n_{\nu} > 0$. Note that for each \mathbf{n} , $F_{\mathbf{n}}(\mathbf{p})$ is nonzero only for a few \mathbf{p} 's. Thus it is better to store a list of \mathbf{p} s with nonzero $F_{\mathbf{n}}(\mathbf{p})$ for each \mathbf{n} and a list of $F_{\mathbf{n}}(\mathbf{p})$ value accordingly. Once these are set up, $D_{\mathbf{n}}$ can be calculated very fast.

With Eqs. 3, 4 and 12, we can now discuss the criterion to determine near and far cell pairs which is crucial in the first downward pass (step 1). Suppose we truncate the terms after the p_m^{th} order. The error is of the order $r^{p_m}/(d-r')^{p_m}$ [7], where r, r' are the radius of the source and the field cell and d is the distance between their centers. In our implementation $r \equiv r'$, thus $r^{p_m}/(d-r')^{p_m} = [\alpha/(2-\alpha)]^{p_m}$. Obviously, the series will converge when $\alpha < 1$. Thus a maximum $\alpha_m < 1$ is chosen to determine whether two cells are near to each other. In Sec. III, we will discuss how to choose it optimally.

Finally the smooth part of magnetostatic field is given by:

$$\vec{H}^s = -\nabla V = \sum_{\mathbf{n}} \frac{1}{\mathbf{n}!} V_{\mathbf{n}} \nabla \mathbf{r}^{\mathbf{n}} \tag{15}$$

And sum over pairs in the nearPartner list \mathcal{L} .

$$\vec{H}_i = \vec{H}_i^s + \sum_{j \in \mathcal{L}, j \neq i} \frac{\vec{m}_j - 3(\vec{m}_j \cdot \hat{r}_{ij}) \hat{r}_{ij}}{r_{ij}^3} \tag{16}$$

The total magnetostatic energy $E = -\sum_i \vec{m}_i \cdot \vec{H}_i$ in unit of $\mu_0/4\pi$.

4. Performance Optimization

A benchmark where randomly oriented dipoles are arranged on a simple cubic lattice was adopted to test the performance of our program. All the

results below are averaged over 50 random configurations and performed on an dual Intel P4 3.0GHz with 2G RAM. Fig. 1 demonstrated that the complexity of our program is $\mathcal{O}(n)$, and it begins to outperform the brute-force calculation around $N_c = 1000$. The small deviations from linearity are caused by the change of hierarchy as the size of the systems increases. The two parallel lines with different colors and symbols correspond to two sets of α_m and p_m achieving the same accuracy. The shift between them indicates that there exists an optimal choice of α_m and p_m set for a given accuracy. In the following analysis, we choose a $32 * 32 * 32$ cubic system, but the conclusions are independent of system size unless it is too small.

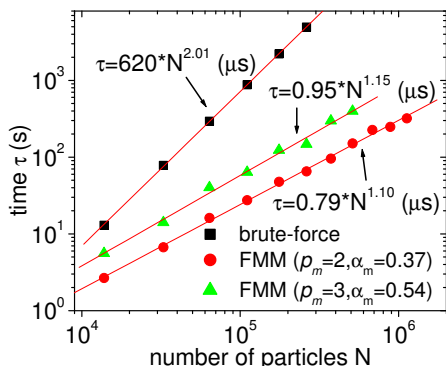


Figure 1: (color online) Computational complexity for the benchmark system. The black square represents the brute-force calculation with complexity $\mathcal{O}(n^2)$, whereas the red dot and green triangles stand for the FMM with two different sets of parameters (α_m, p_m) . The red line is a least square fit to the data.

Before discussing of the parameter set, there is another important issue which affects the performance significantly and needs to be elucidated first. It is the smallest cell size or the average number of particles (s) in the smallest cell. The value of s determines the number of levels in the binary tree and how many brute-force calculations are required on the finest level. Choosing an inappropriate s can deteriorate the performance by a factor of 10. Thus it is indeed a nontrivial issue. Obviously, the larger s is, the fewer levels and the more brute-force calculations will be required. Because of the fairly large overhead of FMM with respect to the brute-force calculation, it is naturally expected that $s = 1$ will not be a good solution. And it is also not good to make s too large, for we will lose the power of the FMM then. So there must be an optimal number s_o which gives best performance for a given

parameter set. Meanwhile, since the overhead increases as the expansion order p_m increases, the optimal s_o is expected to be a function of p_m and should increase with p_m as well. On the other hand, α_m determines the number of cells in the “near” region of each specific cell, but the ratio of the number of cells in the partners list and the number of cells in the nearPartners list should be independent of it. If this ratio remains constant, there is no reason to change s_o for fixed p_m . Therefore, s_o only depends on p_m . Though it is not too difficult to come to this conclusion, it is still not clear at all how to choose s_o . Here, we offer a solution. Table I shows results for a 32^3 system with $p_m = 3$, $\alpha_m = 0.54$. In this case, $s_o = 8$. However as for arbitrary system sizes, we cannot divide them freely, the dependence of s_o on p_m is a discrete function, and different for different system sizes. We overcome this problem by averaging s_o over 30 system size from 30^3 to 59^3 . The result is shown in Fig. 2, where each number beside the square points is s_o for p_m from 2 to 12. The line is a linear fit for those points with $p_m > 3$, indicating an approximate power law relationship between s_o and p_m and the power is approximately 2. As s_o for a given system size will never be the value indicated in the graph anyhow, we reach an empirical equation as follows:

$$s_o = \begin{cases} 0.74p_m^2 & p_m > 3 \\ 8 & otherwise \end{cases} \quad (17)$$

It is very easy to use this equation to estimate s_o . Lastly, for the same s_o , one can have different divisions of the system, but it is always better to have the smallest cell as close to a cube as possible.

Table 1: Performance for ($p_m = 3$, $\alpha_m = 0.54$)

s	$time$
1	34.82
2	14.69
4	8.28
8	6.58
16	9.13
32	13.69
64	20.58

Based on above discussion, we propose a rule of thumb on how to choose the smallest cells: (i) calculate s_o according to Eq. 17; (ii) the smallest

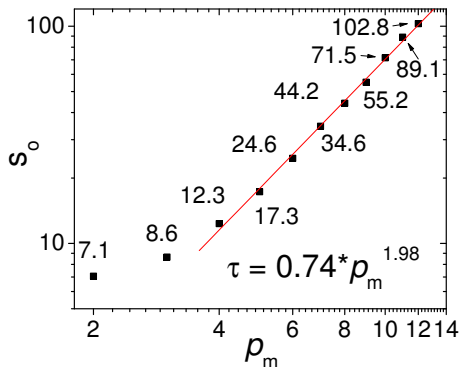


Figure 2: (color online) The optimal number of particles in the smallest cell s_o as a function of expansion order p_m . The red line is fitted by the data ($p_m > 3$). The number next to each data point is the actual s_o .

cells do not have to be cubic and should contain as close to s_o particles as possible; (iii) under the above two conditions, the smallest cells should be as close to cubic as possible. For example: (i) for 50^3 system with $p_m = 3$, the best smallest cell choice is $1.5625 \times 1.5625 \times 3.125$ where each cell on average contains 7.63 particles; (ii) for $40 \times 40 \times 10$ with $p_m = 4$, the best choice is $2.5 \times 2.5 \times 2.5$ (~ 15.6); (iii) for 32^3 with $p_m = 5$, the best choice is $2 \times 2 \times 4$ (~ 16).

Table 2: Performance for $e = 0.05$

p_m	α_m	time
2	0.36	14.15
3	0.54	6.71
4	0.64	6.80
5	0.71	6.22
6	0.76	7.36
7	0.79	8.14
8	0.81	10.65

Now that we know how to divide the system, we can optimize the parameter set (p_m, α_m) . Use $e \equiv [\alpha_m / (2 - \alpha_m)]^{p_m}$ as the error estimate. Obviously, the error decreases as p_m increases and α_m decreases. To achieve certain accuracy, one can have various sets of (p_m, α_m) combinations. The computational effort, on the other hand, increases as p_m increases and α_m decreases. This claim is easy to understand for p_m , since larger p_m results in more terms

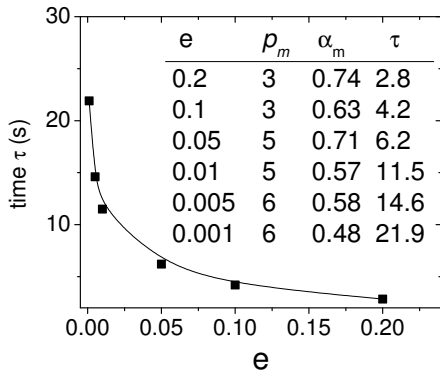


Figure 3: Optimal computing time versus accuracy. The curve is a guide for the eye. The inset table shows the optimal choice of parameter set (p_m, α_m) and the corresponding computing time for each error e .

in the expansion. α_m , on the other hand, determines how many cells there will be in the partners list and nearPartner list. The smaller it is, the more cells there are in the lists, resulting in more computing effort. Therefore the computing effort varies for different sets of (p_m, α_m) . Table II shows one example for $e = 0.05$. Obviously, the choice of $(p_m = 5, \alpha_m = 0.71)$ is optimal in this case. The inset table in Fig. 3 gives the optimal choices of (p_m, α_m) for different accuracies. The curve shows the optimal computing time as a function of accuracy. The computing time grows exponentially when $e < 0.05$, so it suggests to choose $e = 0.05$ if the error is acceptable. In fact, the error of magnetostatic energy for $e = 0.05$ is less than 1% except for configurations whose energy are close to zero. This already reaches the requirement of micromagnetics where other uncertainties may make it pointless to go beyond such accuracy. Thus $(p_m = 5, \alpha_m = 0.71)$ is suggested, if no other requirements exist. Even if higher accuracies are required, $(p_m = 6, \alpha_m = 0.48)$ will definitely be sufficient, since the average percentage error in this case will be 0.02%. Thus, the inefficiency caused by Cartesian coordinates is always less than 2.

Finally we compare the performance of the Cartesian coordinate FMM (CCFMM) with that of the spherical harmonics FMM (SHFMM) and the FFT method. For SHFMM, we use the same tree hierarchy as our CCFMM so that all the performance difference attributes to the difference of base function in expansion: CCFMM uses simple polynomial expansion, while SHFMM uses spherical harmonics, which is much more computationally ex-

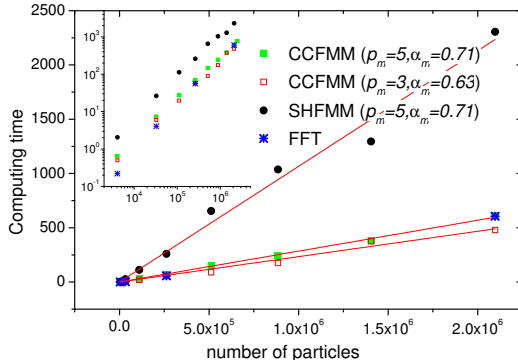


Figure 4: (color online) Comparison of performance of Cartesian coordinate FMM (CCFMM) (green solid square: $p_m = 5, \alpha_m = 0.71$; red open square: $p_m = 3, \alpha_m = 0.63$), spherical harmonics FMM (SHFMM)(black dot: $p_m = 5, \alpha_m = 0.71$) and FFT method (blue star). The inset is a log scale plot. Using Cartesian coordinates makes the FMM roughly three times faster. With $p_m = 5, \alpha_m = 0.71$, the performance of CCFMM is comparable to the FFT method. When the system is sufficiently large or lower accuracy is satisfactory, CCFMM can be superior to FFT.

persive. Regarding the error boundary, these two methods is very similar as long as we keep the parameter set $\{s, p_m, \alpha_m\}$ the same. They will only differ by a small factor of order 1. As to FFT, the routine given in *Numerical Recipes* [16] is used. The results are summarized in Fig. 4. As expected, the computing time increases linearly for both FMM, and the FFT method gives a typical $\mathcal{O}(N * \log(N))$ scaling behavior, which can be seen more clearly on the log scale plot. Focusing on the two FMM, CCFMM is clearly superior to SHFMM. This is all due to the expensive calculation of trigonometric functions of spherical harmonics. Further, cumbersome complex number calculations are avoided by working in Cartesian coordinates. The gain is approximately a factor of three given the chosen parameters. This result is comparable to what has been reported in previous literature[8]. However, differences arise because we use a higher expansion order ($p_m = 5$) while earlier authors used ($p_m = 4$). As a rule of thumb: the higher the order, the less favorable the cartesian expansion. Another factor that results in different speed-ups is the method used to calculate spherical harmonics. In our case, we hard-code the expression of spherical harmonics rather than using recursion relations. Meanwhile we have also minimized the trigonometric functions evaluations. With these optimization of SHFMM though, we found the CCFMM clearly exhibits superior performance at relatively lower

expansion ($p_m < 8$). To achieve a decent 1% average error, parameter set $\{p_m = 5, \alpha_m = 0.71\}$ is recommended. In this case, the performances of FFT and CCFMM are similar. Both the benefit and limitation of FFT is clear. It is an exact method, and it is easy to implement. However, FFT requires a uniform simple cubit grid and a large padding area for exotic structures with open boundary condition. Even though special FFTs can be adapted to nonuniform systems, they become problem specific and complicated. FMM, on the other hand, is quite generic and natural for nonuniform systems and exotic structures with open boundary condition. What's more, it can beat FFT when only lower accuracy is needed, as shown by the red open square in Fig.4.

5. Conclusions

In conclusion, we have implemented and analyzed the performance of the Cartesian coordinate based FMM in dipolar systems. A brief description of the algorithm and supplementary equations are provided. In particular, we present a simple formula (Eq. 3) to calculate the multipole moments for point dipoles. While carefully analyzing the performance by comparing with spherical harmonics FMM and FFT, we have shown that the Cartesian coordinate based FMM is appropriate for magnetic simulations due to their moderate accuracy requirements. A rule of thumb to decide the optimal number of dipoles in the smallest cell is proposed (Eq. 17), and the optimal choices of the expansion order and opening angle under different precision requirements are discussed. ($p_m = 5, \alpha_m = 0.71$) is suggested for nanomagnetic simulation generally. As the FMM is a parallel scalable algorithm, it can be efficiently implemented in parallel architectures.

Acknowledgement: We would like to thank Aiichiro Nakano and Yaqi Tao for useful discussions. The computing facility was generously provided by the University of Southern California high-performance supercomputing center. We also acknowledge financial support by the Department of Energy under grant DE-FG02-05ER46240.

A. APPENDIX

Here we provide the pseudocode for the three recursive function mentioned in Sec. II. Within the framework of object-oriented programming, all

these function are public members of an object called “cell”.

```
void cell::createPartners()
  FOR each cell “A” in the “Partners” list
    IF the cell A is near to this cell THEN
      IF this cell has child THEN
        put the children of A into the “Partners” list of the children of this
        cell;
        erase A from the Partners list of this cell;
      ELSE
        Put A into the NearPartners list of this cell;
        erase A from the Partners list of this cell;
      END IF
    END IF
  END FOR
  IF this cell has child THEN
    put one of its children into the “Partners” list of the other children (do
    this for both children);
    call its children’s CreatePartners();
  ELSE
    Add this cell into the NearPartners list of itself;
  END IF
END FUNCTION
```

```
void cell::updateMoment()
  clear the multipole moments of this cell;
  IF this cell is not the smallest cell Then
    call its children’s updateMoment();
    sum over its children’s multipole moment with shift of origin;
  ELSE IF there is dipoles in this smallest cell THEN
    calculate the multipole moments of this cell directly from the dipole
    distributions;
  END IF
END FUNCTION
```

```
double cell::updateField()
  IF this cell has parent THEN
    inherit the Taylor expansion from its parent with shift of origin;
```

```

END IF
FOR each cell in the "Partners" list
  add to the Taylor expansion of this cell the field generated by A;
END FOR
IF this cell has child THEN
  call its children's updateField();
  calculate the total energy of this cell by the sum of the energy of its
  children;
ELSE
  calculate smooth local field from the Taylor expansion contributed from
  all far cells;
  FOR each cell "A" in the "nearPartners" list
    add to the local field from each dipoles in A except when the dipole
    is located at the field point;
  END FOR
  calculate the energy of this cell by summing over all the dipole in it and
  divide the energy by 2 to eliminate double inclusion of the interaction
  energy
END IF
return the energy of this cell;
END FUNCTION

```

References

- [1] K. De'Bell, A. B. Maclsaac, J. P. Whitehead, *Rev. Mod. Phys.* 72(1) (2000) 225.
- [2] J. I. Martin, J. Nogues, K. liu, J. L. Vicent, I. K. Schuller, *J. Magn. Mater.* 256 (2003) 449.
- [3] S. D. Bader, *Rev. Mod. Phys.* 78 (2006) 1.
- [4] P. Ilg, M. Kroger, *Phys. Rev. E* 72 (2005) 031504.
- [5] M. Shliomis, M. Mond, K. Morozov, *Phys. Rev. Lett* 101 (2008) 074505.
- [6] C. Seberino, H. N. Bertram, *IEEE Trans. Magn.* 37 (2001) 1078.

- [7] P. B. Visscher, D. Apalkov, Simple recursive cartesian implementation of fast multipole algorithm. <http://bama.ua.edu/~visscher/mumag/cart.pdf> (6/10/2008) (2003).
- [8] G. Brown, T. C. Schulthess, D. M. Apalkov, P. B. Visscher, IEEE Trans. Magn. 40 (2004) 2146.
- [9] N. L. Gorn, D. V. berkov, J. Magn. Mater. 272 (2004) 698.
- [10] L. Greengard, The Rapid Evaluation of Potential Fields in Particle Systems, Cambridge, U. K.: MIT Press, 1988.
- [11] L. Greengard, V. Rokhlin, J. Comp. Phys. 73 (1987) 325.
- [12] S. Ogata, T. Campbell, R. Kalia, A. Nakano, P. Vashishta, S. Vemparala, Comput. Phys. Commun 153 (2003) 445.
- [13] J. D. Jackson, Classical Eledrodynamics, Wiley, 3rd Edition, 1999, p. 195.
- [14] J. Shimada, H. Kaneko, T. Takada, J. Comput. Chem. 15 (1994) 28.
- [15] M. Chalacombe, E. Schwegler, J. Almlof, Chem. Phys. Lett. 241 (1995) 67.
- [16] W. H. Press, S. A. Teukolsky, W. T. Vetterling, B. P. Flannery, Numerical Recipes in C++, Cambridge University Press, 2nd Edition, 2002, p. 528.